研究论文

DOI: 10.12211/2096-8280.2025-037

木聚糖酶Xyn11A与阿拉伯呋喃糖苷酶Abf62A协同水解麦秆木聚糖生物合成低聚木糖

胡蝶，徐道铸，鲁志毅，唐卫，樊博，何玉财
（常州大学，药学院 生物与食品工程学院，江苏 常州 213164）

摘要：低聚木糖（XOSs）是一类由2～7个木糖分子通过β-1,4糖苷键连接而成的功能性寡糖，被公认为具有益生元活性的可溶性膳食纤维。在温和条件下的酶催化从廉价生物质提取木聚糖制备高附加值低聚木糖引起了广泛关注。本研究从宇佐美曲霉中克隆了一种阿拉伯呋喃糖苷酶Abf62A基因，并实现其在毕赤酵母X33中的异源表达。利用木聚糖酶Xyn11A（300 U/g底物）和阿拉伯呋喃糖苷酶Abf62A（20 U/g底物）对高浓度麦秆木聚糖（100 g/L）进行协同酶水解，生成50.32 g/L低聚木糖，相较于木聚糖酶Xyn11A单酶水解（34.42 g/L低聚木糖）展现了显著的协同效应。协同水解低聚木糖产物分析结果显示50.32 g/L低聚木糖中包含木二糖（31.71 g/L）、木三糖（15.92 g/L）、木四糖（1.65 g/L）和木五糖（1.04 g/L），其中木二糖和木三糖的含量高达94.7%。此外，从纯化后酶解低聚木糖产物显示可有效清除自由基，抗氧化活性>90%。综上所述，本研究通过木聚糖酶和阿拉伯呋喃糖苷酶Abf62A的协同生物催化作用，以绿色可持续的方式从麦秆木聚糖中制备低聚木糖，为人类和动物健康提供了一种益生元寡糖。

文关键词：阿拉伯呋喃糖苷酶；木聚糖酶；低聚木糖；木聚糖；生物合成

中图分类号：Q814　　**文献标志码：**A

Biosynthesis of xylo-oligosaccharides from wheat straw xylan through the synergistic hydrolysis by xylanase Xyn11A and arabinofuranosidase Abf62A

HU Die，XU Daozhu，LU Zhiyi，TANG Wei，FAN Bo，HE Yucai
（*School of Pharmacy & School of Biological and Food Engineering*，*Changzhou University*，*Changzhou 213164*，*Jiangsu*，*China*）

Abstract: Xylo-oligosaccharides (XOSs) are a category of functional oligosaccharides primarily composed of 2-7 xylose units linked by β-1,4 glycosidic bonds. They are recognized as soluble dietary fibers with prebiotic properties.

收稿日期：2025-04-29 修回日期：2025-07-03
基金项目：国家自然科学基金（22208031，21978072，22308034）
引用本文：胡蝶，徐道铸，鲁志毅，唐卫，樊博，何玉财. 木聚糖酶Xyn11A与阿拉伯呋喃糖苷酶Abf62A协同水解麦秆木聚糖生物合成低聚木糖[J]. 合成生物学，2025，6(4)：972-986
Citation：HU Die，XU Daozhu，LU Zhiyi，TANG Wei，FAN Bo，HE Yucai. Biosynthesis of xylo-oligosaccharides from wheat straw xylan through the synergistic hydrolysis by xylanase Xyn11A and arabinofuranosidase Abf62A[J]. Synthetic Biology Journal，2025，6(4)：972-986

Recently, there has been significant interest in manufacturing XOSs from xylan extracted from lignocellulosic biomass using enzyme catalysis under mild conditions. In this work, the arabinofuranosidase Abf62A gene was cloned from *Aspergillus usamii* genomic DNA through sequential molecular processes and expressed in *Pichia pastoris* X33. The xylan (100 g/L) extracted xylan in wheat straw (WS) was biologically hydrolyzed into 50.32 g/L of XOSs by xylanase Xyn11A (300 U/g substrate) and arabinofuranase Abf62A (20 U/g substrate), which indicated a notable synergistic effect compared to the 34.42 g/L XOSs produced *via* Xyn11A. The 50.32 g/L of XOSs products comprised xylobiose (31.71 g/L), xylotriose (15.92 g/L), xylotetraose (1.65 g/L) and xylopentaose (1.04 g/L). Notably, the combined content of xylobiose and xylotriose accounted for up to 94.7%. The XOSs purified from the enzyme hydrolysate could effectually scavenge free radicals, and the antioxidant activity was more than 90%. In summary, XOSs were biologically manufactured from wheat straw xylan through the synergistic biocatalysis via xylanase and arabinofuranosidase Abf62A in a green and sustainable way, rending one kind of prebiotic oligosaccharides with substantial positive effects on human and animal health.

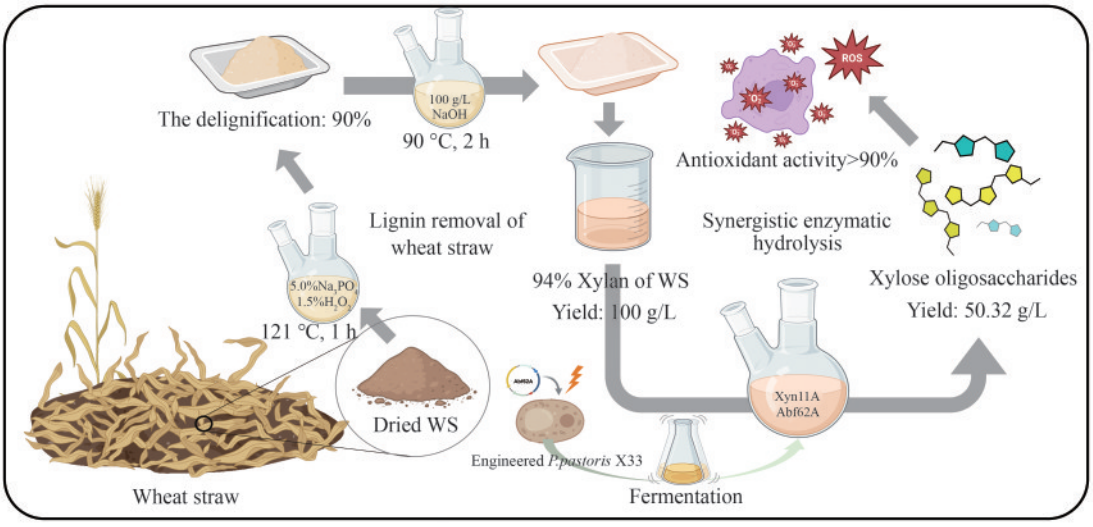

Keywords: arabinofuranosidase; xylanase; xylo-oligosaccharides; xylan; biosynthesis

Xylo-oligosaccharides （XOSs） are sugar oligomers composed of xylose units linked by β-1，4-xylose glycoside bonds. The food and pharmaceutical industries are interested in these carbohydrates because of their probiotic activity， particularly those with a degree of polymerization （DP） ranging from 2 to 6[1]. In its report， the International Scientific Association for Probiotics and Prebiotics defined XOSs as a probiotic oligosaccharide[2]. XOSs have been extensively utilized in food， feed， medical and agricultural fields. They were used as functional food ingredients， supplements， and food additives within the food industry. In addition， XOSs have a low calorie and a certain degree of sweetness， making them as ideal sweeteners for patients with diabetes[3]. In the field of feed， XOSs can enhance nutrient absorption and resistance， and improve animal intestinal flora， so they may be an excellent substitute for antibiotics[4]. As a probiotic in the medical field， XOSs can selectively promote the growth of beneficial bacteria and regulate human intestinal flora[5]. In addition， XOSs have the functions of enhancing immunity， preventing inflammation， and preventing cancer. In

agriculture， XOSs can promote plant growth， improve the soil ecosystem， and enhance the resistance of plants to harsh environments[6].

XOSs can be produced by hydrolysis of xylan[7-8]. Among the sources of xylan， corncob and sugarcane fiber were currently the only lignocellulose biomass used for GRAS-certified commercial XOSs production[1]. Several other wastes from the food industry， such as wheat straw， rice straw， and switchgrass were also used to develop and produce XOSs. Compared with corncob （15%−18% xylan， A/X ratio 0.25−0.35） and sugarcane bagasse （12%−15% xylan）[1]， wheat straw contains higher xylan content （18%−22%） with lower arabinose substitution （A/X= 0.12）[8]， making it more suitable for enzymatic XOS production through reduced arabinofuranosidase requirements. In 2020， the global wheat output was about 760 million tons， and 0.85 g dry straw was produced per gram of wheat， which was an important by-product after harvest[9-10]. Most of them were used for soil fertility， livestock feed and burning to produce energy. By contrast， wood pulp production in the same year was about 184 Mt[11]. Nevertheless， only a small portion of wheat straw （WS） were used as bio-based materials， pulping and fermentation biorefining feedstocks[12]. The effective utilization of WS holds great promising in improving the economy based on rural agriculture.

Currently， the common approaches to prepare XOSs from lignocellulose were acid hydrolysis， self-hydrolysis， enzymatic hydrolysis or their combination[13]. While the cost of self-hydrolysis was high and undesired impurities could be generated in the lignocellulose processing[14]. The reaction conditions of acid hydrolysis to generate XOSs were harsh， and the degree of hydrolysis was not easy to control， resulting in difficult separation and purification of the product and low yield[15]. Enzymatic digestion is a promising method to produce XOSs because of its mild reaction conditions， few by-products， environment-friendly and easy to control[16]. Acid hydrolysis typically achieves <40% XOS yields due to uncontrolled xylose depolymerization[17]. Enzymatic hydrolysis achieves 60%−80% XOS yields under mild conditions （50−60 ℃， pH 4−6）， avoiding toxic byproducts like furfural and acetic acid common in acid methods[1]. However， the current scale and yield of XOSs produced by xylanase direct enzymatic hydrolysis are still very limited， and thus combining enzymatic methods with other techniques is essential to improve the yield and purity of XOSs. Hemicellulose with high purity can be acquired by physical or chemical methods to improve the binding efficiency of xylanase and/or xylan[17-18]. In addition， there were many groups connected to the side chain （*e.g.*， arabinose group， galactose group， gluconic acid group） of xylan in biomass， and these groups also influence the enzymatic hydrolysis of xylanase. The xylan in wheat straw primarily exists in the form of arabinoxylan， whose structure is composed of a β-1，4-xylose main chain and α-L-furanosyl arabinose side chains. The arabinose/xylose ratio in wheat straw arabinoxylan is 1∶10. Arabinose is linked to the xylose residues of the xylan backbone through α-1，2 or α-1，3 glycosidic bonds， forming a branched structure[19] The α-L-arabinofuranosidases （EC 3.2.1.55）， belong to the glycoside hydrolase （GH） familie GH62， are a kind of glycoside hydrolase enzyme that specifically catalyzes the hydrolysis of α-L-arabinofuranosidic bonds. It targets and cleaves arabinose residues linked as side chains in complex carbohydrates， such as arabinoxylan， arabinan， or pectin[20]. It has been proven that the breakdown of arabinose substituents can alleviate steric hindrance in arabinoxylan， provide additional binding sites for xylanase， and significantly enhance xylanase hydrolysis efficiency. The synergistic effect of α-L-arabinofuranosidases and other glycoside hydrolases demonstrates their significant role and

great potential in industrial biotechnology.

In this research, the xylan in WS was chemoenzymatically converted into XOSs through the sequential extract with solvent and biocatalysis with hydrolase. The arabinofuranosidase gene Abf62A was cloned from *Aspergillus usamii* genomic DNA, and expressed in *Pichia pastoris* X33. The solvent containing Na_3PO_4 and H_2O_2 were used to pretreat WS. Then, the high purity xylan was extracted, and the enzymatic hydrolysis of xylan was studied systematically, including the effect of lignin and arabinosyl elimination on the enzymatic hydrolysis of XOSs, and the antioxidant activity of XOSs after desalting and decolorization. This work aimed to develop an effective strategy for manufacturing XOSs from biomass, realizing the high-value utilization of biomass.

1 Materials and methods

1.1 Strains, vectors, materials

The *A. usamii* E001, isolated from the soil in China as reported previously, was used as the donor of Abf62A[18]. The *Escherichia coli* DH5α competent cell and yeast expression vector pPICZαA used for the construction of the recombinant expression vectors, and the *P. pastoris* X33 (Novagen, Madison, WI, USA) was for recombinant expression strain. The hybrid Xyn11A, a family 11 xylanase from *A. usamii* E001, was expressed in *P. pastoris* GS115, and Xyn11A was harvested as previous reported[18]. The straw samples were from Puyang, Henan Province. The bleomycin were purchased from Sigma-Aldrich (St. Louis, MO, USA). The standard samples of xylose, arabinose and galactose were purchased from China National Medicines Corporation Ltd.

1.2 Extraction of xylan from wheat straw

The crushed or preteated (by 5% Na_3PO_4 and 1.5% H_2O_2 at 121 ℃ for 1 h) wheat straw were soaked with 10% (by mass) NaOH solution at 90 ℃ for 2 h, and the solid-to-liquid mass ratio was 1∶10. The treated liquor's pH was regulated to 5.0 with concentrated HCl, and a 3-folds volume of 95% ethanol was added to this liquor to obtain xylan precipitation, which was collected through vacuum filtration, washed with water and 70% ethanol, and then oven-dried at 60 ℃. The remaining xylan solids were washed to neutral with distilled water and oven-dried at 60 ℃. The xylan extracted from untreated wheat straw contained 7.3% cellulose, 79.9% hemicellulose and 10.6% lignin. The xylan extracted from pretreated wheat straw contained 3.1% cellulose, 94% hemicellulose and 1.2% lignin.

1.3 Cloning and expression of arabinofuranosidase Abf62A in *P. pastoris*

The arabinofuranosidase gene Abf62A was cloned from *A. usamii* genomic DNA. Initial PCR amplification was performed using degenerate primers Abf-F (5′-atgaaattcctcaaagccaaggg-3′) and Abf-R (5′-tcactgcttcaaggtaagaactcc-3′), generating a 999-bp fragment containing the native secretion signal. The secretion signal was subsequently removed by redesigning the primers (Abf62A-F: 5′-aaatgcgctcttccgtcgac-3′ and Abf62A-R: 5′-tcactgcttcaaggtaagaactcc-3′) to produce a mature 918-bp coding sequence. The truncated gene fragment, amplified with primers containing pGAPZαA homology arms, was recombined with the pGAPZαA vector through homologous recombination to generate the 3952-bp plasmid pGAPZαA-Abf62A. The recombinant plasmid was transformed into *E. coli* DH5α for propagation and confirmed by DNA sequencing. The verified plasmid was then linearized at the AvrII site using the primers Avr-F (5′-ggacggtaacgggcggtggaaggagagagaaggga-3′) and Avr-R (5′-ctaggaaattttactctgctggagagcttcttctac-3′), electroporated into *P. pastoris* X33, and screened on bleomycin resistant YPD plate to construct the engineered strain X33/pGAPZαA-

Abf62A.

For enzyme expression， a single colony of *P. pastoris* X33/pGAPZαA-*Abf62A* strain grown on YPD agar was inoculated into 2 mL of YPD medium in a 10 mL test tube. The culture was incubated overnight at 30 ℃ with 200 r/min orbital shaking. Subsequently， 1 mL of the seed culture was inoculated into 100 mL of YPD medium in a 500 mL flask. The culture was incubated for 72 h under optimum conditions （30 ℃， pH 5.5） with 0.5% methanol induction. After incubation， the culture was centrifuged at 8000×*g* for 5 min. The supernatant was collected and filtered through a 0.22 μm membrane. The resulting solution was stored at 4 ℃ for further analysis.

1.4 Enzyme activity assay of arabinofuranosidase

The 10 g/L wheat xylan solution was immersed in sodium acetate buffer （50 mmol/L， pH 5.0） at 50 ℃ for 10 min. Using 10 g/L wheat xylan as the standard， the amount of reducing sugar liberated was quantified by the 3，5-dinitrosalicylic acid （DNS） method under the assay conditions （at pH 5.0 and 60 ℃ for 15 min）. The solution after enzymatic hydrolysis was diluted properly， 0.5 mL diluted solution was mixed with 0.5 mL DNS solution. The mixture was incubated for 7 min in boiling water bath and cooled and eventually 1 mL distilled water was supplemented to determine the UV absorption value of 540 nm. One unit （U） of enzyme activity was defined as the amount of enzyme that catalyzes the liberation of 1 μmol of reducing sugars per min.

1.5 Purification and enzymatic properties of arabinofuranosidase Abf62A

The Abf62A fermentation liquor was filtered through a 0.45 μm membrane and loaded onto a nickel ion affinity column （PC002HiTalon IMAC-μSphere， 5 mL bed volume）. The column was eluted at a flow rate of 5 mL/min with a mobile phase consisting of 20 mmol/L Tris-HCl and 500 mmol/L NaCl （pH 7.4）， and the effluent was collected. The target protein adsorbed on the column was then eluted with a solution containing 200 mmol/L imidazole at the same flow rate. The eluate solution was concentrated using a 10 kDa ultrafiltration tube at 5000×*g* for 20 min. The buffer was exchanged multiple times by centrifugation with a solution of 20 mmol/L sodium phosphate buffer （pH 5.5） to obtain the purified Abf62A solution.

The optimum medium pH and reaction temperature value of purified Abf62A were determined through the measurement of reducing sugar under the standard arabinofuranosidase activity assay conditions， except at designed the pH values from 3.5 to 8.0 and temperatures from 30 ℃ to 80 ℃ in 100 mmol/L sodium phosphate buffer. To evaluate the pH stability and thermostability， the purified Abf62A was incubated in the absence of substrate at the different pH values and temperatures for 1 h. Then， the enzyme activity was measured under the optimum reaction conditions using 10 g/L wheat xylan as the substrate.

1.6 Detection of XOSs by HPLC analysis

The HPLC analysis with refractive index detector was used to quantify xylose and XOSs with DP≤6. The sample was eluted by Rezex RSO-Oligosaccharide Ag^+ （4%） （200 mm×10 mm） chromatography column （Phenomenex， USA） and guard column （60 mm×10 mm）. The mobile phase was 3 mL/min degassed Milli-Q water. The temperatures of detector and column were 40 ℃ and 85 ℃， respectively. All samples were centrifuged with 7000 r/min for 10 min and filtered through a 0.22 μm pore size disposable filter.

1.7 Analysis of antioxidant activity of XOSs

The XOS hydrolysate obtained under optimized

synergistic enzymatic conditions was desalted and decolorized using strongly basic anion-exchange and sodium-form cation-exchange resins. The solution was concentrated to half volume by rotary evaporation at 50 ℃ and lyophilized to obtain solid XOSs samples. For antioxidant assays, XOS and ascorbic acid (VC) solutions (1−10 g/L) were prepared with distilled water as blank. Radical scavenging activity was calculated as: Scavenging (%)=(A_0-A_1)/A_0×100%, where A_0 and A_1 represent blank and sample absorbance, respectively. DPPH radical scavenging was measured by mixing 100 μL sample with 100 μL 0.16 mmol/L DPPH, incubating at 25 ℃ for 15 min, and reading absorbance at 517 nm. ABTS assay involved combining 20 μL sample with 200 μL 0.16 mmol/L ABTS, incubating in darkness at 25 ℃ for 1 h, then measuring absorbance at 734 nm. Hydroxyl radical scavenging was determined by adding 200 μL sample to 200 μL 9 mmol/L $FeSO_4$ and 200 μL 9 mmol/L ethanolic salicylic acid, initiating with 200 μL 0.01% H_2O_2, incubating at 37 ℃ for 1 h, and reading at 510 nm. Superoxide anion scavenging was assessed by pre-incubating 100 μL sample with 300 μL Tris-HCl buffer (pH 8.0) at 25 ℃ for 20 min, adding 100 μL 5 mmol/L HCl-pyrogallol, reacting for 5 min, terminating with 100 μL 100 mmol/L HCl, and measuring absorbance at 325 nm.

2 Results and discussion

2.1 Recombinant expression of Abf62A in *P. pastoris* X33

The arabinofuranosidase gene *Abf62A* was successfully cloned from *A. usamii* and expressed *in P. pastoris* [Fig. 1(a) and (b)]. Electrophoretic analysis confirmed the removal of the native secretion signal, yielding a mature 918-bp coding sequence [Fig.1(c)]. Homologous recombination generated the 3952-bp plasmid pGAPZαA-*Abf62A*, which was subsequently transformed into *P. pastoris* X33. SDS-PAGE of culture supernatants revealed distinct ~33 kDa protein bands [Fig.1(d)], consistent with Abf62A's predicted molecular mass (32.8 kDa). Optimum enzyme production occurred at 30 ℃ and pH 5.5 with 0.5% methanol induction.

Using the wheat xylan solution of 10 g/L as the substrate, the protease activity was detected. The results were showcased in Fig. 2. It was obvious that three strains had higher protease activity. The highest protease activity was 10 U/mL, and the lowest protease activity was 5 U/mL. Consequently, strain 4 was selected for subsequent culture optimization.

2.2 Optimization of culture conditions of X33/pGAPZαA-*Abf62A*

The strain 4 with the highest enzyme activity was selected to optimize the culture conditions. As showcased in Fig. 3(a), the enzyme activity of Abf62A was ow with 36 h, implying that *P. pastoris* was in the cell growth period, with less protein expression and low enzyme activity. Subsequently, the enzyme activity increased continuously, and the enzyme activity reached the highest at 66 h. However, the enzyme activity began to decline instead of rising for 72 h. The decline in enzyme activity beyond 66 h is attributed to proteolytic degradation during prolonged fermentation, a well-documented phenomenon in *P. pastoris* systems [21]. While protein aggregation may contribute to activity loss, protease-mediated hydrolysis is recognized as the primary factor for heterologous protein instability in late-phase cultures [21]. Therefore, 66 h was established as the optimal cultivation period to maximize functional enzyme yield.

The cell growth and cell metabolism of *P. pastoris* will be substantially influenced by temperature. As showcased in Fig.3(b), the enzyme activity of Abf62A expressed at 24−36 ℃ basically increased gradually, acquiring the highest at 30 ℃, and then declined with the increase of

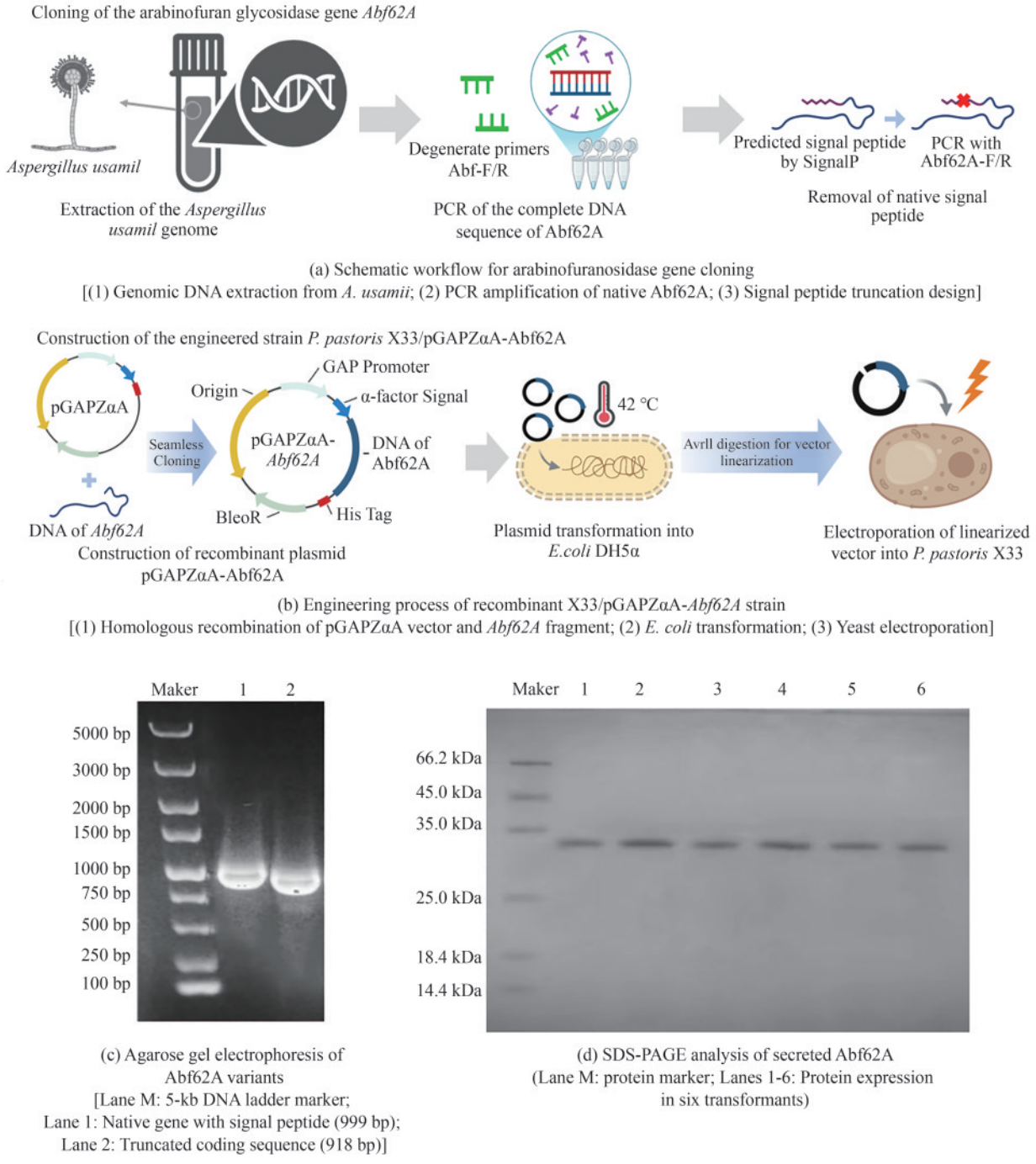

Fig. 1 Cloning and expression analysis of Abf62A in *P. pastoris*

reaction temperature， but the enzyme activity of Abf62A expressed at 26 ℃ was also very high as 94.3%， which was due to the inconsistency between the optimum growth temperature of *P. pastoris* and the optimum temperature for protein expression. The optimum temperature for yeast growth was generally 30 ℃， while the suitable temperature for protein expression was lower， between 20 ℃ and 28 ℃. At 30 ℃， the expression of natural protein was high. While the protein expression of single yeast was high at 26 ℃， but the cell concentration was low， which led to a small difference in enzyme activity of Abf62A

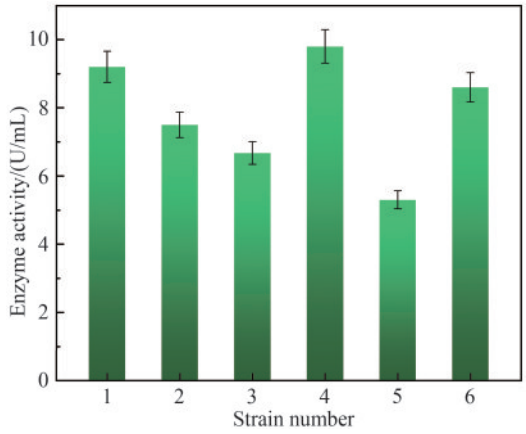

Fig. 2 Abf62A enzyme activity of different strains

cultured at these two temperatures. Accordingly, the appropriate culture temperature was 30 ℃.

2.3 Purification and characterization of Abf62A

The specific enzyme activity of Abf62A fermentation liquor expressed under optimization of culture conditions was 14.9 U/mL (or 159.0 U/mg protein), which was 43% higher than that of control (10 U/mL). It could be seen from Fig. 4 lane A that there were some number of miscellaneous proteins in the crude enzyme solution of Abf62A, but there was also Abf62A in the flow-through fluid (Fig. 4 lane B), indicating that the target proteins Abf62A didn't bind to the chromatographic column well during the chromatography process. For all this, the Abf62A eluate solution was purified to electrophoretic purity (Fig. 4 lane C). After ultrafiltration concentration of Abf62A eluate solution, the specific enzyme activity of Abf62A pure enzyme solution (Fig. 4 lane D) was 347.9 U/mL (or 173.5 U/mg protein).

As showcased in Fig. 5(a), it was observed that the enzyme activity of Abf62A varies greatly between pH 3.5 and 8.0. When the pH was between 5.0 and 6.0, the enzyme activity was higher than 80%, and the optimum pH was pH 5.5. However, the enzyme activity under other pH was very low. Especially, the enzyme activity of Abf62A was only less than 10% when the pH was alkaline. This was due to the fact that the enzyme was derived from fungi and the optimum pH was usually in the acidic range [22]. The arabinofuranosidase Abf4980 screened from *Bispora* sp. MEY-1CGMCC2500 and expressed in *P. pastoris* GS115 manifested good activity in pH 3.0−6.0 [22-23]. The stability of Abf62A between pH 5.0−6.0 was excellent, all above 90%, and the enzyme activity was above 60% under acidic condition. In contrast, the enzyme activity under alkaline conditions was very low, and the remaining enzyme activity after incubation at pH 8.0 for 1 h was less than 20%. This might be caused by enzyme inactivation under alkaline conditions. The arabinoxylanase from *Bacillus subtili* was also the most stable in pH under pH 5.5 [24]. However, the pH stability of enzymes from other strains varies greatly, and α-L-arabinosidase in *Jiangella alba*

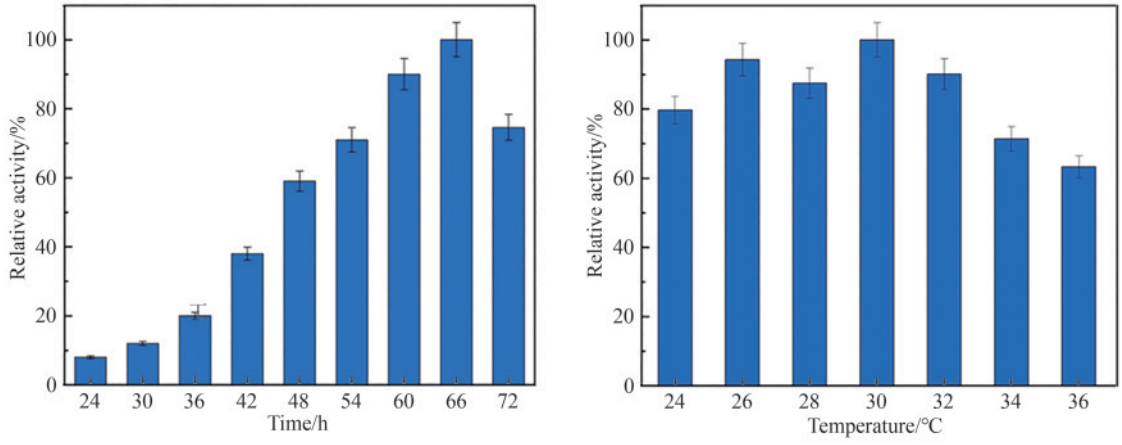

Fig. 3 Effects of culture time (a) and temperature (b) on the enzyme activity of Abf62A fermentation liquor.

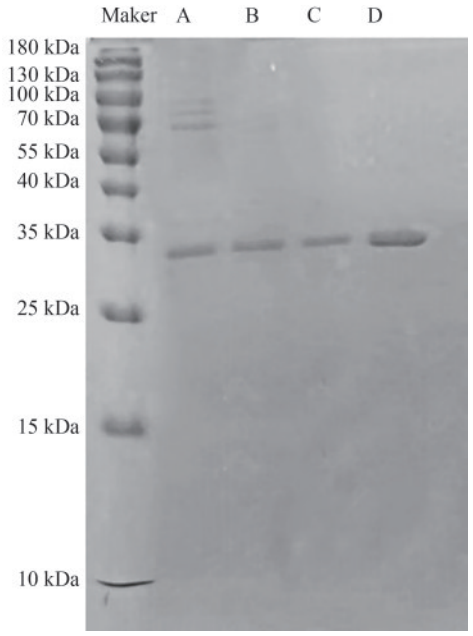

Fig. 4 SDS-PAGE results Abf62A protein

(Lane A: Abf62A fermentation liquor; Lane B: Abf62A flow-through solution; Lane C: Abf62A eluate solution; Lane D: Abf62A pure enzyme solution)

DSM45237 still maintained high activity under the condition of pH 8.0 [25].

Under the optimum pH conditions, the enzyme activity of arabinofuranosidase Abf62A at different temperatures was assessed. The results were showcased in Fig. 5（b）. It was found that the optimum temperature of Abf62A was 60 ℃, and the enzyme activity declined sharply as the temperature continued to rise. 63% of enzyme activity was acquired at 65 ℃, and less than 10% at 80 ℃. Too high temperature can cause the protein denaturation, which would result in the rapid decrease of enzyme activity [25]. α-L-arabinofuranosidase from *A. terreus* was heterologous expressed in *P. pastoris* X33 and remained stable at 60−65 ℃, which was consistent with the results of this research [26]. In addition, it was obvious that the temperature stability of Abf62A was poor. The enzyme activity reached the maximum at 30 ℃, and the enzyme activity weakened gradually with the increase of temperature, but the remaining enzyme activity was 81% at 55 ℃. After rising to 60 ℃, the enzyme activity was maintained only 50%. Almost all the enzymes were denatured at 80 ℃, and the enzyme activity was only 2.4%. The newly discovered α-L-arabinofuranosidase Abf4980 remained fully active after incubation at 70 ℃ for 24 hours, showing excellent thermal stability [23]. At present, industrial applications are pursuing enzymes with high temperature stability [27-29]. Directional mutagenesis is one of the most powerful tools for improving the biophysical properties of proteins for biopharmaceutical and industrial processes [30-32], which can be used to further improve the thermostability of Abf62A.

2.4 Hydrolytic products analyses of wheat straw xylans by Xyn11A

Recently, there is great interest to manufacture

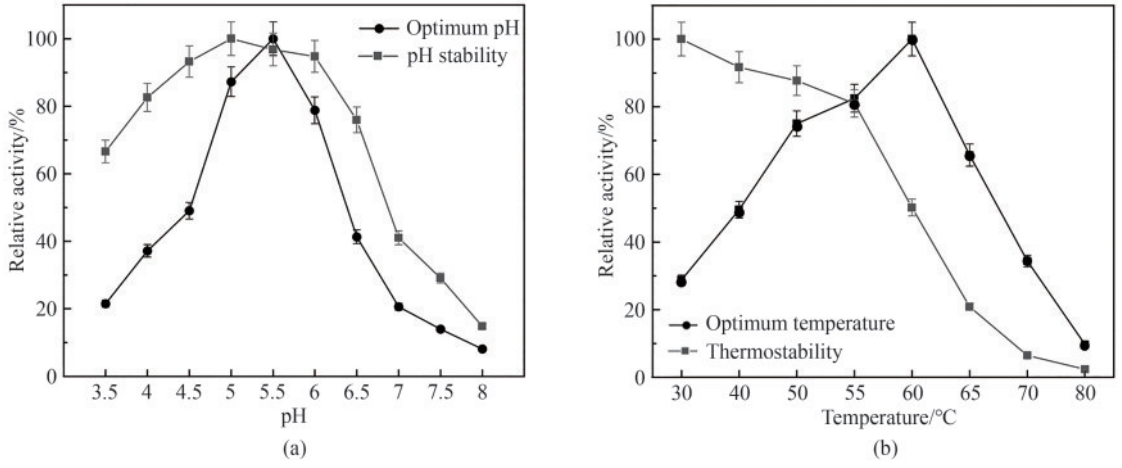

Fig. 5 The optimum pH and pH stability of Abf62A (a) and its optimum temperature and temperature stability (b)

XOSs from biomass in a benign and sustainable way [1, 33-34]. The integrated biorefinery process from wheat straw to XOSs is schematically illustrated in Fig. 6. The wheat straw was determinand to contain 42.86% cellulose, 26.83% hemicellulose, and 22.95% lignin. Following delignification (90% efficiency) through optimized alkaline peroxide pretreatment (5% Na_3PO_4, 1.5% H_2O_2, 121 ℃, 1 h), the cellulose-enriched residue of wheat straw was subjected to further extract xylan with 96.9% recovery by NaOH method. Xylanase can hydrolyze xylan formed by the interconnection of xylan molecules, but other components in xylan will substantially influence the hydrolysis of xylan. The xylans extract from unpretreated (UTX) and pretreated (PTX) wheat straw were used as substrates for the enzyme hydrolysis by Xyn11A, and the results were displayed in Table 1. The Xylan (100 g/L) was mixed with xylanase (Xyn11A of 200 U/g substrate) and incubated at 70 ℃ and pH 5.0 for 6 h. It was observed that there was slight difference in the proportion of various sugars to total sugars in these two xylan-hydrolysates, but there was a substantial difference in concentration. After the enzyme hydrolysis of UTX, the total sugar concentration was 21.12 g/L. Among them, a total content of xylose, XOSs and arabinose was 20.77 g/L, and the hydrolysis efficiency of purified xylan was 26% (the xylan content in UTX was 79.9%). Through the enzymolysis of PTX, the total sugar content reached 36.62 g/L. It was detected that the content of XOSs was 34.42 g/L, including xylobiose (20.85 g/L), xylotriose (11.44 g/L), xylotetraose (1.13 g/L), and xylpentaose (1.0 g/L). The hydrolysis

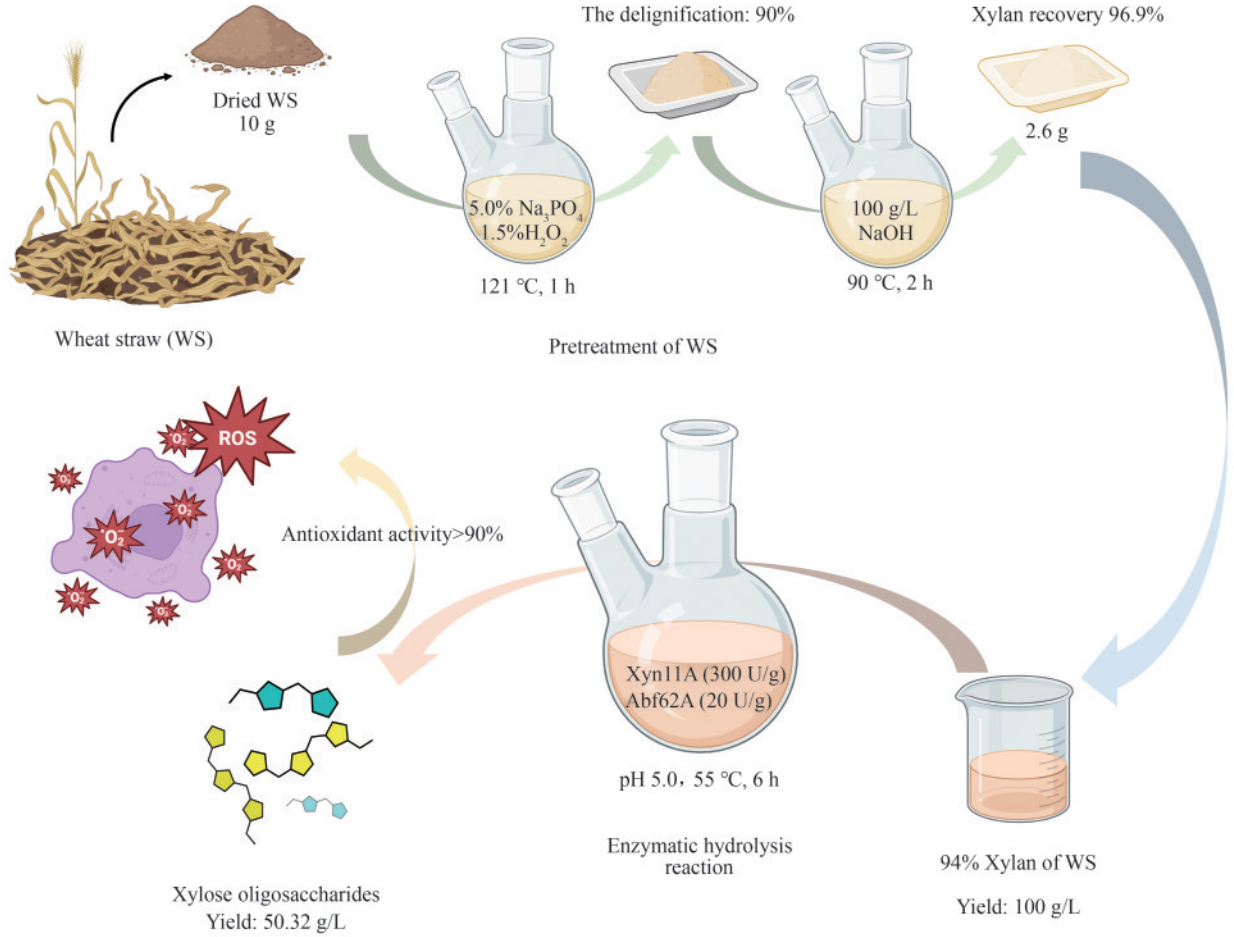

Fig. 6 Integrated process for valorizing wheat straw into antioxidant xylooligosaccharides

Table 1 Analysis of Xyn11A enzymatic hydrolysis products of different WS xylan

Product	UTX		PTX	
	Concentration/(g/L)	Proportion/%	Concentration/(g/L)	Proportion/%
Xylose	0.63	3.08	1.37	3.97
Xylobiose	11.69	57.16	20.85	60.45
Xylotriose	7.61	37.21	11.44	33.17
Xylotetraose	0.41	2.01	1.13	3.28
Xylopentaose	0.26	1.27	1.0	2.90
Arabinose	0.17	0.83	0.43	1.25
Glucose	0.35	1.71	0.4	1.16

efficiency of xylan was 39% （the content of xylan in PTX was 94%）. The difference of enzymatic hydrolysis results between them might be due to their difference of lignin content [35]. Component analysis indicated that the main difference of xylan extracted from WS before （10.6% lignin） and after （1.2% lignin） pretreatment was the content of lignin. Direct extraction of xylan from WS retained a large amount of lignin， produce irreversible adsorption to the enzyme in the process of hydrolysis， reduce enzyme activity， and the lignin-carbohydrate complex structure formed by the combination of lignin and xylan will hinder the combination of xylanase and xylan， resulting in xylanase cannot play a role.

2.5 Hydrolytic products analyses of wheat straw xylans by Xyn11A and Abf62A

The synergistic enzymatic hydrolysis of wheat straw xylan by Xyn11A and Abf62A yielded substantial XOS production， with detailed compositional analysis presented in Table 2. The reaction conditions were as follows： The Xyn11A of 300 U/g substrate and Abf62A of 20 U/g substrate were supplemented to the solution containing 100 g/L of xylan and reacted at 55 ℃ and pH 5.0 for 6 h. Under the synergistic enzymatic hydrolysis under optimum conditions， the total sugar content from the hydrolysis of UTX was 23.45 g/L. Compared with the results of enzymatic hydrolysis without Abf62A， the sugar concentration had no apparent increase. The Abf62A had little influence on assisting Xyn11A. Due to the direct extraction of xylan without pretreatment， other components in UTX， mainly cellulose （7.3%） and lignin （10.6%） may produce irreversible adsorption with the enzyme in the process of enzymatic hydrolysis， which greatly reduced the activity of the enzyme. In contrast， the results of enzymatic hydrolysis of PTX with Xyn11A and Abf62A were entirely different. All sugar contents were greatly increased. The content of XOSs reached 50.32 g/L， including xylobiose （31.71 g/L）， xylotriose （15.92 g/L）， xylotetraose （1.65 g/L） and xylopentaose （1.04 g/L）. Compared with the results of enzymatic hydrolysis without Abf62A， the

Table 2 Sugar content and proportion in xylan hydrolysates of different WS

Product	UTX		PTX	
	Concentration/(g/L)	Proportion/%	Concentration/(g/L)	Proportion/%
Xylose	0.55	2.35	1.43	2.63
Xylobiose	12.38	52.79	31.71	58.22
Xylotriose	8.35	35.61	15.92	29.23
Xylotetraose	0.62	2.64	1.65	3.03
Xylopentaose	0.47	2.01	1.04	1.91
Arabinose	0.62	2.64	2.34	4.30
Glucose	0.46	1.96	0.38	0.70

xylobiose content increased 10.86 g/L. The above results showcased that WS samples before and after pretreatment had a great influence on the subsequent enzymatic saccharification of xylan. The content of XOSs produced by PTX enzymatic hydrolysis was much higher than that of UTX, in which the proportion of DP2-5 XOSs was more than 92%, which was the main factor affecting the probiotic effect of XOSs. The color value of PTX was also much lower than that of UTX, which greatly reduced the purification steps of XOSs, saved operation time and performance cost. The synergy between Xyn11A and Abf62A stems from complementary roles: Abf62A removes arabinose substitutions at xylan's *O*-2/*O*-3 positions, reducing steric hindrance and enabling Xyn11A to efficiently cleave β-1,4-glycosidic bonds. Lignin removal during pretreatment further minimizes non-productive enzyme binding. This mechanism aligns with prior studies demonstrating that arabinose debranching enhances xylan accessibility [36].

2.6 Analysis of antioxidant activity of XOSs

As probiotics, the antioxidant activity of XOSs is an important evaluation index [37]. Fig. 7(a) and Fig. 7(b) manifested the ABTS and DPPH radical scavenging rates of VC, UT-XOS and PT-XOS (XOSs obtained from the hydrolysis of UTX and

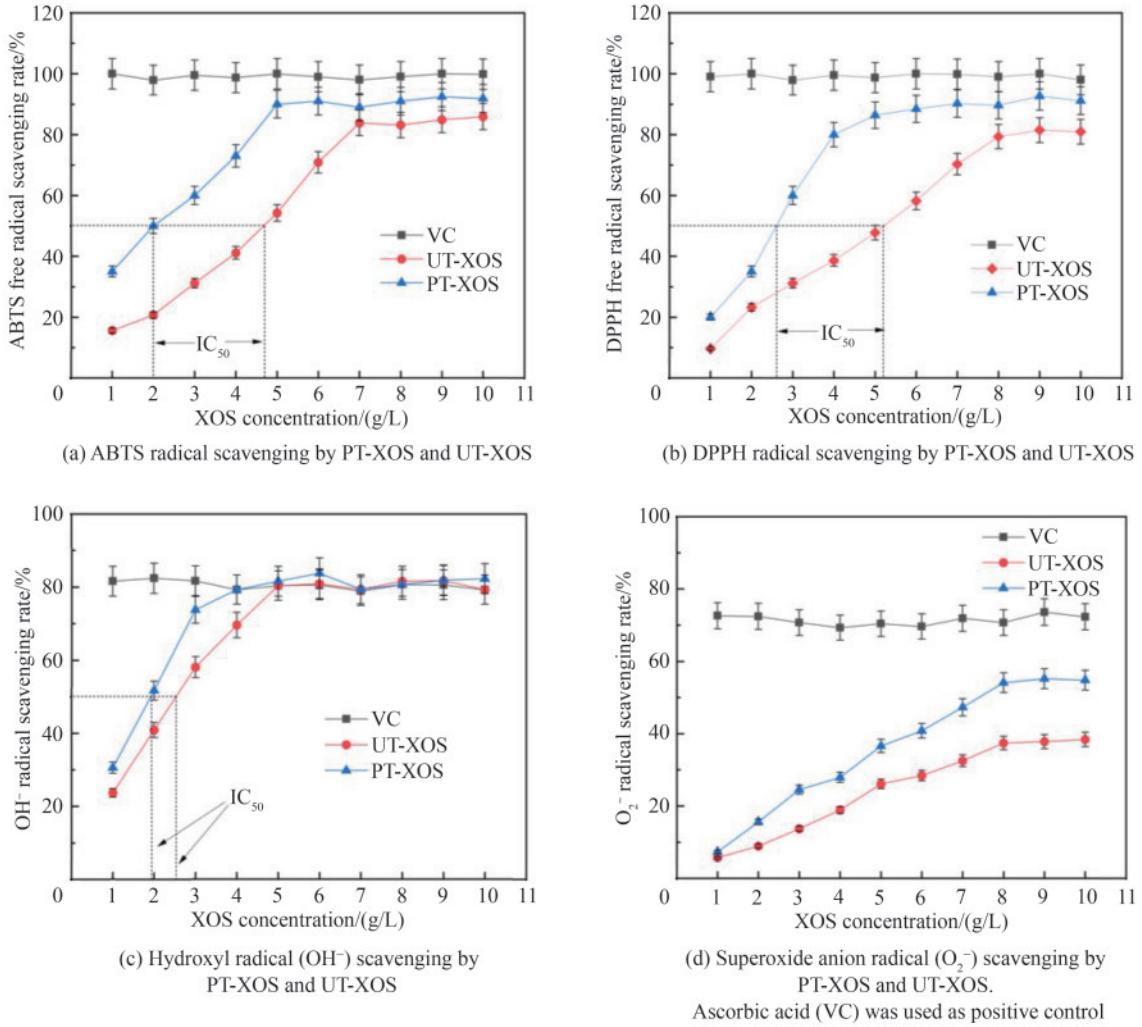

(a) ABTS radical scavenging by PT-XOS and UT-XOS

(b) DPPH radical scavenging by PT-XOS and UT-XOS

(c) Hydroxyl radical (OH^-) scavenging by PT-XOS and UT-XOS

(d) Superoxide anion radical (O_2^-) scavenging by PT-XOS and UT-XOS.
Ascorbic acid (VC) was used as positive control

Fig. 7 Radical scavenging activity of xylo-oligosaccharides (XOS)

(Data represent mean values of triplicate measurements.)

PTX by Xyn11A and Abf62A）. The free radical scavenging ability of these two kinds of XOSs was proportional to the concentration to a certain extent. With elevating concentration of XOSs， the free radical scavenging rates of ABTS and DPPH were also gradually increasing， but both were weaker than VC. The IC_{50} values of PT-XOS and UT-XOS to ABTS free radical were 1.99 g/L and 4.68 g/L respectively， and the IC_{50} values of PT-XOS and UT-XOS to DPPH free radical were 2.6 g/L and 5.2 g/L， respectively， which was much higher than that of UT-XOS， because the purity of PT-XOS was higher than that of UT-XOS. In the ABTS free radical scavenging experiment， the highest free radical scavenging rate of UT-XOS was about 84%， and that of PT-XOS was about 90%. There was no substantial difference between them， but the amount of XOSs used was higher than that of PT-XOS by 2 g/L. A similar situation occurred in the DPPH experiment. When PT-XOS content was 5 g/L， the scavenging rate of DPPH free radicals was 86.4%， almost reaching the maximum value. While the free radical scavenging rate of the same concentration of UT-XOS was only 47.8%， the free radical scavenging rate of 8 g/L reached the maximum value of about 80%， which was also lower than UT-XOS. Higher purity reduces lignin-derived phenolics that quench free radicals[11]， while increased DP2-4 proportion exposes more reducing ends for electron donation[34].

OH^- free radicals and O_2^- free radicals have the ability to oxidize many biological macromolecules in the human body[38]， including nucleic acids， proteins and lipids， which lead to accelerated aging and a variety of diseases. In this work， the scavenging effects of UT-XOS and PT-XOS on OH^- and O_2^- free radicals were further compared ［Fig. 7（c）and（d）］. The two kinds of XOS manifested good scavenging effect on OH^- free radicals. The IC_{50} of UT-XOS and PT-XOS were 2.53 g/L and 1.92 g/L， respectively， and the optimum free radical scavenging rate was similar to that of VC. The scavenging effect of O_2^- free radical was much worse， the highest scavenging rate of PT-XOS was only about 55%， the UT-XOS was even lower， only about 38%， and the concentration requirements of both were much higher than before.

3 Conclusion

In this research， biomass was effectively converted into XOSs *via* a chemoenzymatic cascade way. The extracted xylan from wheat straw （WS） could be biologically hydrolyzed into XOSs by arabinofuranosidase from *A. usamii*. Xylan （100 g/L） could be hydrolyzed into XOSs after enzymolysis with xylanase （Xyn11A 300 U/g substrate） and arabinofuranase （Abf62A of 20 U/g substrate)， and 50.32 g/L of XOSs formed including xylobiose （31.71 g/L)， xylotriose （15.92 g/L)， xylotetraose （1.65 g/L） and xylopentaose （1.04 g/L）. The XOSs purified from the enzyme hydrolysate could effectually scavenge free radicals and had the excellent antioxidant activity. Importantly， this research opened up a new path for the transformation of lignocellulose based on lignin removal and synergistic enzymatic hydrolysis of biomass. Future studies will focus on enhancing enzyme thermostability through protein engineering and optimizing continuous production processes. Exploring the applications of XOS in functional foods represents another promising avenue.

参 考 文 献

[1] SANTIBÁÑEZ L, HENRÍQUEZ C, CORRO-TEJEDA R, et al. Xylooligosaccharides from lignocellulosic biomass: a comprehensive review[J]. Carbohydrate Polymers, 2021, 251: 117118.

[2] GIBSON G R, HUTKINS R, SANDERS M E, et al. Expert consensus document: the International Scientific Association for Probiotics and Prebiotics (ISAPP) consensus statement on the definition and scope of prebiotics[J]. Nature Reviews

Gastroenterology & Hepatology, 2017, 14(8): 491-502.

[3] YAN F, TIAN S Q, DU K, et al. Preparation and nutritional properties of xylooligosaccharide from agricultural and forestry byproducts: a comprehensive review[J]. Frontiers in Nutrition, 2022, 9: 977548.

[4] LIU Z X, LIU M H, MENG J, et al. A review of the interaction between diet composition and gut microbiota and its impact on associated disease[J]. Journal of Future Foods, 2024, 4(3): 221-232.

[5] ZHOU J M, WU S G, QI G H, et al. Dietary supplemental xylooligosaccharide modulates nutrient digestibility, intestinal morphology, and gut microbiota in laying hens[J]. Animal Nutrition, 2021, 7(1): 152-162.

[6] CHEN W W, GUO C, HUSSAIN S, et al. Role of xylo-oligosaccharides in protection against salinity-induced adversities in Chinese cabbage[J]. Environmental Science and Pollution Research, 2016, 23(2): 1254-1264.

[7] CARRILLO I, MENDONÇA R T, AGO M, et al. Comparative study of cellulosic components isolated from different *Eucalyptus* species[J]. Cellulose, 2018, 25(2): 1011-1029.

[8] POLETTO P, PEREIRA G N, MONTEIRO C R M, et al. Xylooligosaccharides: transforming the lignocellulosic biomasses into valuable 5-carbon sugar prebiotics[J]. Process Biochemistry, 2020, 91: 352-363.

[9] KUMAR P, BARRETT D M, DELWICHE M J, et al. Methods for pretreatment of lignocellulosic biomass for efficient hydrolysis and biofuel production[J]. Industrial & Engineering Chemistry Research, 2009, 48(8): 3713-3729.

[10] KUMAR R, PRAKASH O. Experimental investigation on effect of season on the production of bioethanol from wheat-stalk (WS) using simultaneous saccharification and fermentation (SSF) method[J]. Fuel, 2023, 351: 128958.

[11] ZHANG L M, LARSSON A, MOLDIN A, et al. Comparison of lignin distribution, structure, and morphology in wheat straw and wood[J]. Industrial Crops and Products, 2022, 187: 115432.

[12] SUN M X, XU X B, WANG C D, et al. Environmental burdens of the comprehensive utilization of straw: wheat straw utilization from a life-cycle perspective[J]. Journal of Cleaner Production, 2020, 259: 120702.

[13] BRENELLI L B, FIGUEIREDO F L, DAMASIO A, et al. An integrated approach to obtain xylo-oligosaccharides from sugarcane straw: from lab to pilot scale[J]. Bioresource Technology, 2020, 313: 123637.

[14] HIDAYATULLAH I M, AL HUSNA M D, RADIYAN H, et al. Combining biodelignification and hydrothermal pretreatment of oil palm empty fruit bunches (OPEFB) for monomeric sugar production[J]. Bioresource Technology Reports, 2021, 15: 100808.

[15] ZHAO J Y, BIAN B, WANG X K, et al. Integrating ball milling assisted enzymatic hydrolysis of bamboo cellulose for controllable production of xylo-oligosaccharides, monosaccharides and cellulose nanofibrils[J]. Industrial Crops and Products, 2024, 209: 118024.

[16] MANISHA, YADAV S K. Technological advances and applications of hydrolytic enzymes for valorization of lignocellulosic biomass[J]. Bioresource Technology, 2017, 245 (Pt B): 1727-1739.

[17] CARVALHO A F A, DE OLIVA NETO P, DA SILVA D F, et al. Xylo-oligosaccharides from lignocellulosic materials: chemical structure, health benefits and production by chemical and enzymatic hydrolysis[J]. Food Research International, 2013, 51(1): 75-85.

[18] ZHANG H M, LI J F, WANG J Q, et al. Determinants for the improved thermostability of a mesophilic family 11 xylanase predicted by computational methods[J]. Biotechnology for Biofuels, 2014, 7(1): 3.

[19] KULATHUNGA J, ISLAM S. Wheat arabinoxylans: insight into structure-function relationships[J]. Carbohydrate Polymers, 2025, 348: 122933.

[20] WILKENS C, ANDERSEN S, DUMON C, et al. GH62 Arabinofuranosidases: structure, function and applications[J]. Biotechnology Advances, 2017, 35(6): 792-804.

[21] PETUSHKOVA A I, ZAMYATNIN A A. Redox-mediated post-translational modifications of proteolytic enzymes and their role in protease functioning[J]. Biomolecules, 2020, 10(4): 650.

[22] PORIA V, SAINI J K, SINGH S, et al. Arabinofuranosidases: characteristics, microbial production, and potential in waste valorization and industrial applications[J]. Bioresource Technology, 2020, 304: 123019.

[23] LIU X Q, GAO F, WANG Y R, et al. Characterization of a novel thermostable α-L-arabinofuranosidase for improved synergistic effect with xylanase on lignocellulosic biomass hydrolysis without prior pretreatment[J]. Bioresource Technology, 2024, 394: 130177.

[24] YAN R Y, WANG W J, VUONG T V, et al. Structural characterization of the family GH115 α -glucuronidase from *Amphibacillus xylanus* yields insight into its coordinated action with α-arabinofuranosidases[J]. New Biotechnology, 2021, 62: 49-56.

[25] AYTAŞ Z G, TUNÇER M, KUL Ç S, et al. Partial characterization of β-glucosidase, β-xylosidase, and α-L-arabinofuranosidase from *Jiangella alba* DSM 45237 and their potential in lignocellulose-based biorefining[J]. Sustainable Chemistry and Pharmacy, 2023, 31: 100900.

[26] LI P H, YANG C, JIANG Z W, et al. Lignocellulose pretreatment by deep eutectic solvents and related technologies: a review[J]. Journal of Bioresources and

Bioproducts, 2023, 8(1): 33-44.

[27] 康里奇, 谈攀, 洪亮. 人工智能时代下的酶工程[J]. 合成生物学, 2023, 4(3): 524-534.
KANG L Q, TAN P, HONG L. Enzyme engineering in the age of artificial intelligence[J]. Synthetic Biology Journal, 2023, 4 (3): 524-534.

[28] 丁明珠, 李炳志, 王颖, 等. 合成生物学重要研究方向进展[J]. 合成生物学, 2020, 1(1): 7-28.
DING M Z, LI B Z, WANG Y, et al. Significant research progress in synthetic biology[J]. Synthetic Biology Journal, 2020, 1(1): 7-28.

[29] 阮青云, 黄莘, 孟子钧, 等. 蛋白质稳定性计算设计与定向进化前沿工具[J]. 合成生物学, 2023, 4(1): 5-29.
RUAN Q Y, HUANG X, MENG Z J, et al. Computational design and directed evolution strategies for optimizing protein stability[J]. Synthetic Biology Journal, 2023, 4(1): 5-29.

[30] SELLÉS VIDAL L, ISALAN M, HEAP J T, et al. A primer to directed evolution: current methodologies and future directions [J]. RSC Chemical Biology, 2023, 4(4): 271-291.

[31] 祁延萍, 朱晋, 张凯, 等. 定向进化在蛋白质工程中的应用研究进展[J]. 合成生物学, 2022, 3(6): 1081-1108.
QI Y P, ZHU J, ZHANG K, et al. Recent development of directed evolution in protein engineering[J]. Synthetic Biology Journal, 2022, 3(6): 1081-1108.

[32] MCLURE R J, RADFORD S E, BROCKWELL D J. High-throughput directed evolution: a golden era for protein science [J]. Trends in Chemistry, 2022, 4(5): 378-391.

[33] YANG Q Z, FAN B, HE Y C. Combination of solid acid and solvent pretreatment for co-production of furfural, xylooligosaccharide and reducing sugars from *Phyllostachys edulis*[J]. Bioresource Technology, 2024, 395: 130398.

[34] TANG Z Y, FAN B, TANG W, et al. Comprehensive understanding of co-producing fermentable sugar, furfural, and xylo-oligosaccharides through the pretreatment with CTAB-based deep eutectic solvent containing Brønsted and Lewis acid [J]. Chemical Engineering Journal, 2024, 488: 150637.

[35] ALVAREZ V M Z, FERNÁNDEZ P V, CIANCIA M. Structure-antioxidant activity relationship of xylooligosaccharides obtained from carboxyl-reduced glucuronoarabinoxylans from bamboo shoots[J]. Food Chemistry, 2024, 455: 139761.

[36] KRISTENSEN J B, THYGESEN L G, FELBY C, et al. Cell-wall structural changes in wheat straw pretreated for bioethanol production[J]. Biotechnology for Biofuels, 2008, 1(1): 5.

[37] CHEN Y, TANG Z Y, TANG W, et al. Exploration of biomass fractionation and lignin removal for enhancing enzymatic digestion of wheat-stalk through deep eutectic solvent Cetyl trimethyl ammonium chloride: lactic acid treatment[J]. International Journal of Biological Macromolecules, 2025, 306: 141460.

[38] CHANDIMALI N, BAK S G, PARK E H, et al. Free radicals and their impact on health and antioxidant defenses: a review [J]. Cell Death Discovery, 2025, 11: 19.

通讯作者： 何玉财（1979—），男，博士，教授，博士生导师，研究方向为合成生物学和生物质能源。
E-mail：heyucai2001@126. com

第一作者： 胡蝶（1988—），女，博士，助理研究员，硕士生导师。研究方向为酶工程与酶分子设计。
E-mail：Butterflystudy@163. com